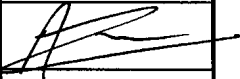

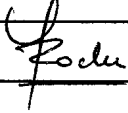
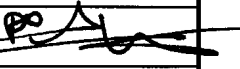


HERSCHEL
Magnetic field of the solar generator

Product Code:

Rédigé par/ Written by	Responsabilité-Service-Société Responsibility-Office -Company	Date	Signature
A.LUC	EMC engineer	22/06/06	
Vérifié par/ Verified by			
P.COUZIN	Electrical Interface Manager	5/9/06	
Approbation/ Approved			
Y.ROCHE	System Manager	07/09/06	
J.J. JUILLET	Project manager	11/09/06	

Entité Emettrice : Alcatel Alenia Space - France
(détentrice de l'original)



HERSCHEL/PLANCK		DISTRIBUTION RECORD	
DOCUMENT NUMBER : H-P-2-ASP-TN-1093		Issue : 1 Date: 08/02/2006	
EXTERNAL DISTRIBUTION		INTERNAL DISTRIBUTION	
ESA	X	HP team	X
ASTRIUM	X		
ALCATEL ALENIA SPACE -Italia			
CONTRAVES			
TICRA			
TECNOLOGICA			
		ClI Documentation	Orig.



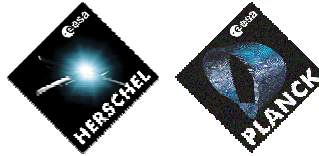
ENREGISTREMENT DES EVOLUTIONS / CHANGE RECORDS

ISSUE	DATE	§ : DESCRIPTION DES EVOLUTIONS § : CHANGE RECORD	REDACTEUR AUTHOR
1	08/02/2006	First issue	LUC A.
2	22/06/2006	Second issue. The magnetic field of each section of the solar array on the PACS cryo-harness has been evaluated.	LUC A.



TABLE OF CONTENTS

1. INTRODUCTION	5
2. REFERENCE DOCUMENT	5
3. MAGNETIC FIELD ANALYSIS	5
3.1 Solar array mechanical layout	5
3.2 Electrical design of the solar array	6
3.3 Power supply regulation principle	8
3.3.1 Variation of the current between operating point and short circuit	8
3.3.2 Transients	8
3.4 Magnetic field evaluation	11
3.4.1 Evaluation of the field generated at the switching frequency	12
3.4.2 Evaluation of the magnetic field generated by the transients	16
4. ANALYSIS	19
5. CONCLUSION	20



1. INTRODUCTION

The aim of this technical note is to provide an evaluation of the magnetic field generated by the Herschel solar array sections on the PACS cryo-harness.

2. REFERENCE DOCUMENT

- [RD 01] : Herschel – Electrical Power Analysis and Design Report , HP-2-GAMI-AN-0014
- [RD 02] : Magnetic moment analysis (Herschel), HP-4-GAMI-AN-0016
- [RD 03] : EMC Specification, H-P-1-ASPI-SP-0037
- [RD 04] : Drawing “Herschel FM side panel 1”, AD-T0067191-00-03, issue3
- [RD 05] : Drawing “Herschel FM side panel 2”, AD-T0067192-00-03, issue3
- [RD 06] : Drawing “Herschel FM side panel 3”, AD-T0067193-00-03, issue3
- [RD 07] : Proposed modification of Herschel Solar Array to reduce H-field emission, H-P-2-ASP-TN-1200

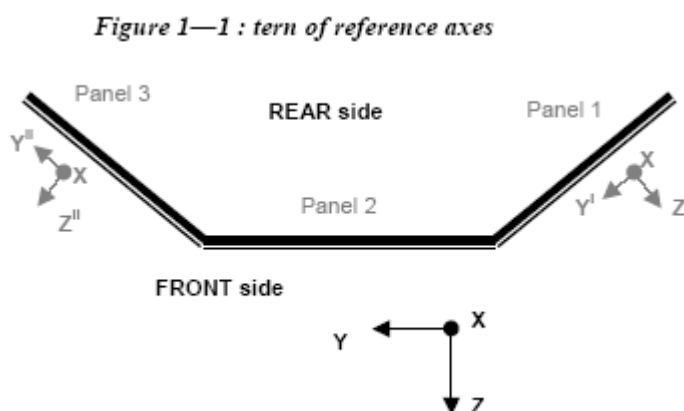
3. MAGNETIC FIELD ANALYSIS

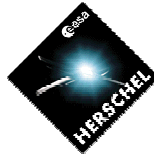
NOTA : all section numbers are those defined in [RD 04], [RD 05] and [RD 06], however the table of § 3.2 gives the correspondence between ASED numbers and Galileo Avionica numbers.

3.1 Solar array mechanical layout

The Herschel mechanical design is presented in annex 1.

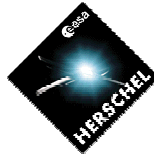
The layout of the panels is as follows:





3.2 Electrical design of the solar array

The following table gives the magnetic moment (calculated by GA, see [RD 02]) of each section in the associated Z direction, i.e. roughly in the direction of the cryo-harness cables.



Section (ASED)	Section (Galileo Avionica)	Magnetic moment (A.m ²)
30	1	-0.115
29	2	0.049
28	3	0.117
27	7	0.099
26	5	-0.066
25	9	-0.055
24	4	-0.072
23	17	-0.015
22	6	0.118
21	10	-0.198
20	14	0.028
19	18	0.063
18	13	-0.522
17	11	0.011
16	15	0.082
15	16	-0.027
14	8	-0.048
13	12	0.053
12	19	-0.129
11	29	0.004
10	21	0.077
9	22	-0.131
8	26	0.11
7	30	0.133
6	25	-0.34
5	23	-0.024
4	27	0.042
3	28	-0.034
2	20	-0.018
1	24	0.038

At every moment only one section is working and consequently generating a non constant magnetic field.

Remark : Each magnetic moment calculated before corresponds to variation of the current associated to the section between 0 and I_{max}. This approach is wrong with the S3R principle since the current is varying between I_{max} (short circuit) and I at operating point.



3.3 Power supply regulation principle

The solar array power is dumped by serial shunt regulators. A solar array section is periodically short circuited in the shunt regulator MOSFET. The periodical signal is pulse width modulated in order to vary the dumped average power. Nominally one shunt is working while the other are fully open or closed.

The current ripple towards the users power bus is filtered by the PCDU capacitor.

3.3.1 Variation of the current between operating point and short circuit

A solar cell acts as a current source with a non linear impedance characteristic.

The solar cell working point is always below the maximum power point since the solar array voltage is regulated to 30 V by shunts. The maximum current variation is $\Delta I = 0.225 \text{ A}$ corresponding to $I_{sc} = 2.14 \text{ A}$ and $I_{oper} = 1.915 \text{ A}$.

3.3.2 Transients

An evaluation of the current transients in the solar array due to the commutation of the S3R has been performed. Measurements and simulations have been performed. Results are presented in annex 2.

Main steps are explained here after :

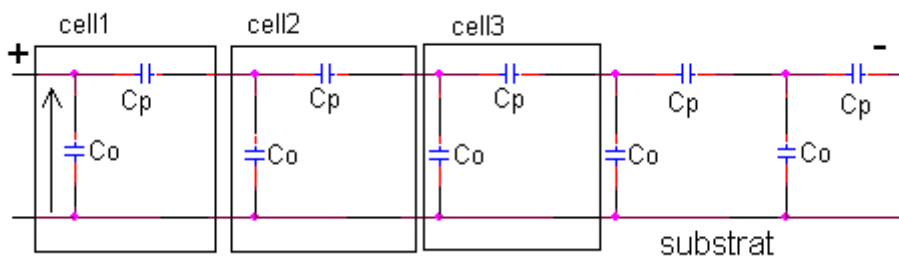
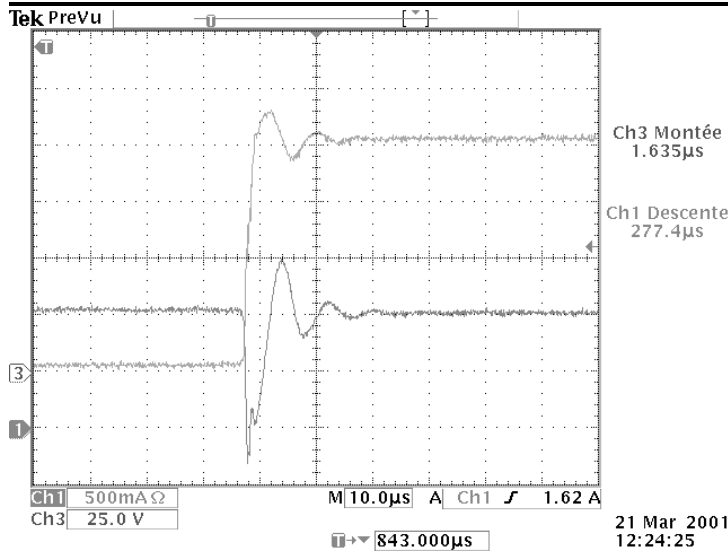


Figure 3.3.2-1 Solar Array string model

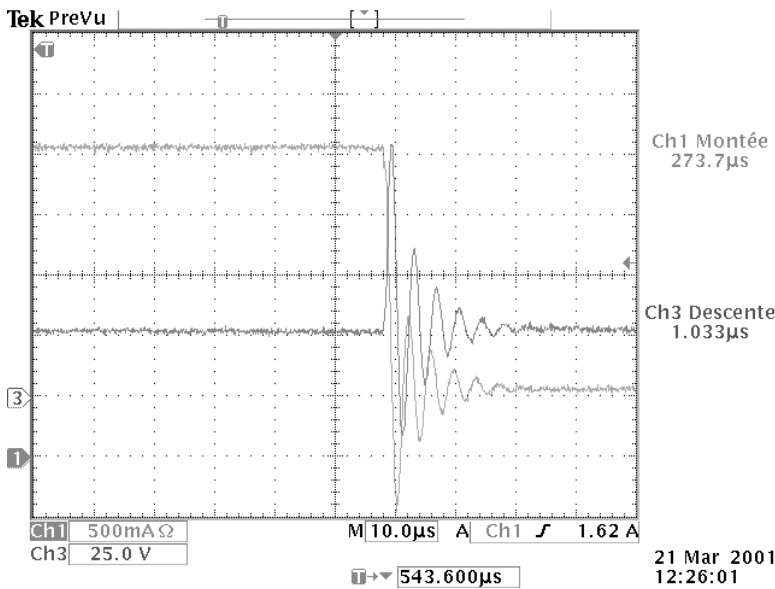
The transients exist either at the opening or at the closing of the shunt :

- At the opening of the shunt, the parasitic capacitances (C_p and C_0) need to be recharged from 0 to 30V . All the current delivered by the solar array cells is consumed by these capacitances, increasing slowly the solar array panel voltage. A weak resonance generates an over current and a voltage transient.



Ch1 : string current (500mA/div)
Ch3 : string voltage (25V/div)

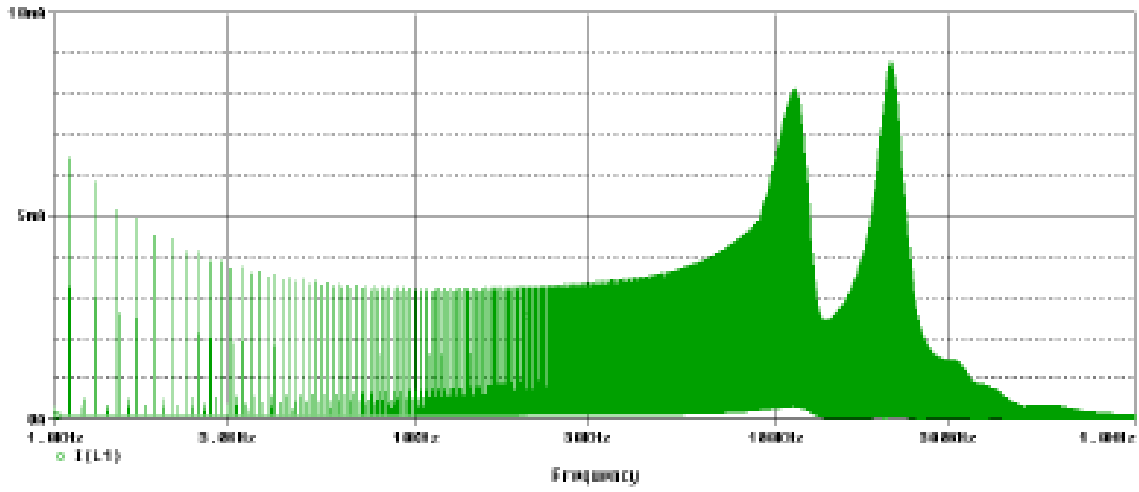
- At the closing of the shunt, the parasitic capacitances discharge through the harness producing a current and voltage oscillations.



Ch1 : string current (500mA/div)
Ch3 : string voltage (25V/div)

Free wheel diode suppresses the oscillations at shunt closure.

Fourier transform performed on the last simulated signal gives the following spectrum (20 samples of the transients have been taken into account):
The results show that the signal is contained between the switching frequency and 150 kHz.





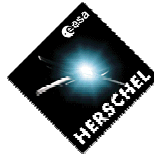
3.4 Magnetic field evaluation

Different points (A,B,C,D,E) of the cryo-harness are considered. Following tables give the positions of these points and of the centre of the solar array section which can be in switching mode.

Point	X	Y	Z
A	2375	-655	703
B	1630	0	946
C	2276	231	922
D	1642	366	877
E	956	1238	1055

SECTION N°	X	Y	Z
24	1,438	0,991	1,669
27	1,438	1,318	1,427
30	1,438	1,642	1,187
21	1,89	1,817	1,058
12	2,316	0,991	1,669
15	2,316	1,318	1,427
18	2,316	1,642	1,187
6	2,987	1,195	1,518
9	2,987	1,666	1,17
3	3,307	1,195	1,518
20	1,455	0,535	1,835
23	1,455	0,233	1,835
26	1,455	-0,079	1,835
29	1,455	-0,42	1,835
8	2,351	0,535	1,835
11	2,351	0,233	1,835
14	2,351	-0,079	1,835
17	2,351	-0,42	1,835
22	1,438	-0,991	1,669
25	1,438	-1,318	1,427
28	1,438	-1,642	1,187
19	1,89	-1,817	1,058
10	2,316	-0,991	1,669
13	2,316	-1,318	1,427
16	2,316	-1,642	1,187
4	2,986	-1,195	1,518
1	3,306	-1,195	1,518
7	2,986	-1,666	1,17

Nota : section 2 and 5 located on the upper part (+X) of the panels have not been considered.



Evaluation of the field produced by a loop :

B is the magnetic field which is equal to the sum of two field components Bx and Br

Bx is the magnetic field component on the coil axis and Br the component in the radial direction

I is the current in the wire

R is the radius of the current loop

D₁ is the distance on axis from the centre of the current loop to the point which is considered

D₂ is the radial distance from the axis of the current loop to the point which is considered

$$B_x = (I \cdot \mu_0) / (2 \cdot \pi \cdot R) \cdot 1 / (\text{sqr}Q) [E(k) \cdot (1 - \alpha^2 - \beta^2) / (Q - 4\alpha) + K(k)]$$

$$B_r = (I \cdot \mu_0) / (2 \cdot \pi \cdot R) \cdot \gamma / (\text{sqr}Q) [E(k) \cdot (1 + \alpha^2 + \beta^2) / (Q - 4\alpha) - K(k)]$$

With

$$\alpha = D_2 / R$$

$$\beta = D_1 / R$$

$$\gamma = D_1 / D_2$$

$$Q = (1 + \alpha)^2 + \beta^2$$

K(k) and E(k) are elliptic integral functions

$$\mu_0 = 4\pi \cdot 10^{-7}$$

Value of D1 and D2 for point E with regard to the centre of the section 30

$$D_1 = 0.294 \text{ m}$$

$$D_2 = 0.512 \text{ m}$$

3.4.1 Evaluation of the field generated at the switching frequency

3.4.1.1 Magnetic field of Section 30 at point E

Considering the maximum current variation is $\Delta I = 0.225 \text{ A}$ (see § 2.3.1) at section level.



Section 30 is constituted of 5 strings :

Section	String	Area main (m ²)	Area redundant (m ²)
30	42	-0.121	-0.038
	43	-0.082	0.120
	44	-0.054	0.143
	45	-0.008	0.226
	46	0.152	0.264

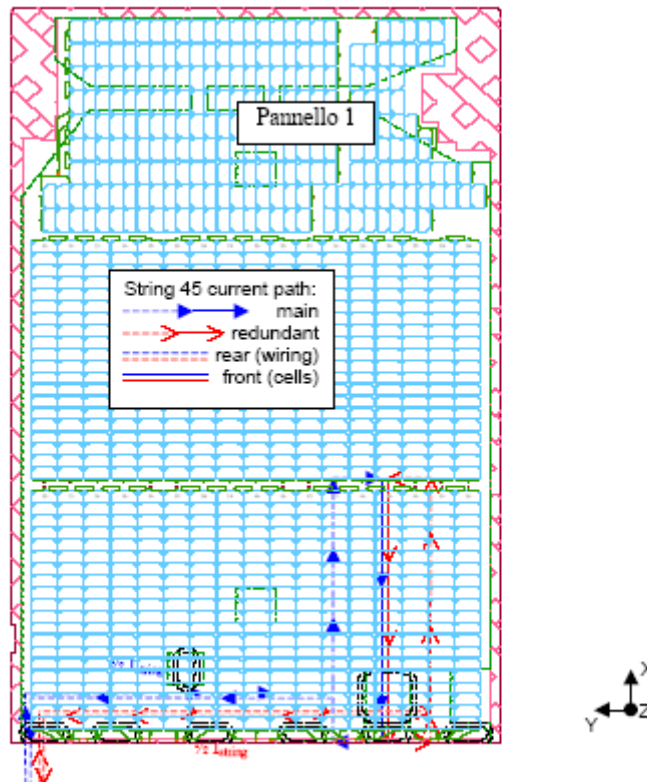


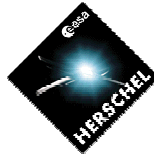
Figure 2.4.1-1 : String 45, typical current path (extracted from [RD 02])

The variation of the current at string level is $0.225/5 = 0.045$ A and at half string level 0.0225 A.

The total loop area obtained by adding the string area (main and redundant) is 0.602 m²

This area is equivalent to a loop with a radius of 0.44 m

The evaluation of the field generated by section 30 at point E level is performed taking into account the following values :



$$I = 0.0225 \text{ A}$$

$$R = 0.44 \text{ m}$$

$$D1 = 0.294 \text{ m}$$

$$D2 = 0.512 \text{ m}$$

The result is $B_x = 3.42 \text{ nT}$ and $B_r = 10.07 \text{ nT}$

Field amplitude is $B = 10.7 \text{ nT}$ i.e. 81 dBpT

Nota 1: The magnetic field evaluation taking into account each string individually gives a similar value of $B = 11.2 \text{ nT}$

Nota 2 : The contribution of the AWG20 twisted wires has been considered as negligible.

3.4.1.2 Magnetic field of Section "X" at point "Y"

All fields have been evaluated following the same approach as in § 3.4.1.1.

The following table presents the results :



Section N°	Point	D1 (mm)	D2 (mm)	I (A)	R (m)	Bx (10 ⁻⁹ T)	Br (10 ⁻⁹ T)	B (10 ⁻⁹ T)	B dBpT
24	E	289	799	0.0225	0.24	0.43	0.71	0.83	58
27	E	291	535	0.0225	0.24	0.3	2.6	2.62	68
30	E	294	512	0.0225	0.44	3.42	10.07	10.7	81
18	E	294	1371	0.0225	0.3	0.21	0.15	0.26	48
21	E	299	1011	0.0225	0.33	0.52	0.63	0.82	58
21	D	1015	1081	0.0225	0.33	0.11	0.35	0.37	52
18	C	1058	970	0.0225	0.3	0.15	0.31	0.35	51
15	C	1056	568	0.0225	0.35	0.65	0.55	0.85	59
12	C	1053	165	0.0225	0.28	0.81	0.18	0.83	59
9	C	1059	1226	0.0225	0.28	0.04	0.2	0.21	47
6	C	1055	822	0.0225	0.41	0.46	0.66	0.81	58
3	C	1055	1110	0.0225	0.41	0.17	0.49	0.52	55
20	B	889	563	0.0225	0.15	0.16	0.18	0.24	48
23	B	889	291	0.0225	0.17	0.42	0.21	0.47	54
26	B	889	192	0.0225	0.35	1.8	0.52	1.88	66
29	B	889	455	0.0225	0.07	0.05	0.04	0.06	35
11	C	913	2	0.0225	0.11	0.22	0.001	0.22	47
8	C	913	313	0.0225	0.24	0.72	0.37	0.81	58
14	C	913	319	0.0225	0.18	0.41	0.22	0.47	54
17	C	913	655	0.0225	0.13	0.09	0.12	0.15	44
25	A	977	942	0.0225	0.7	1.11	1.75	2.07	67
22	A	974	987	0.0225	0.44	0.31	0.74	0.80	58
28	A	979	1062	0.0225	0.22	0.05	0.17	0.18	45
10	A	974	316	0.0225	0.53	2.44	0.97	2.62	68
13	A	977	113	0.0225	0.87	4.73	0.46	4.76	74
16	A	979	502	0.0225	0.2	0.29	0.25	0.38	52
4	A	976	614	0.0225	0.32	0.55	0.58	0.80	58
1	A	976	933	0.0225	0.3	0.16	0.38	0.41	52
7	A	980	808	0.0225	0.37	0.41	0.65	0.77	58
19	A	981	865	0.0225	0.43	0.46	0.81	0.93	60



3.4.2 Evaluation of the magnetic field generated by the transients

Simulations have been performed using the model presented in annex 2 and adapted with the following values

Bus voltage : 28 V

Solar array section capacitance : 500 nF

Wiring inductance : 2*2 μ H

Results are presented hereafter :

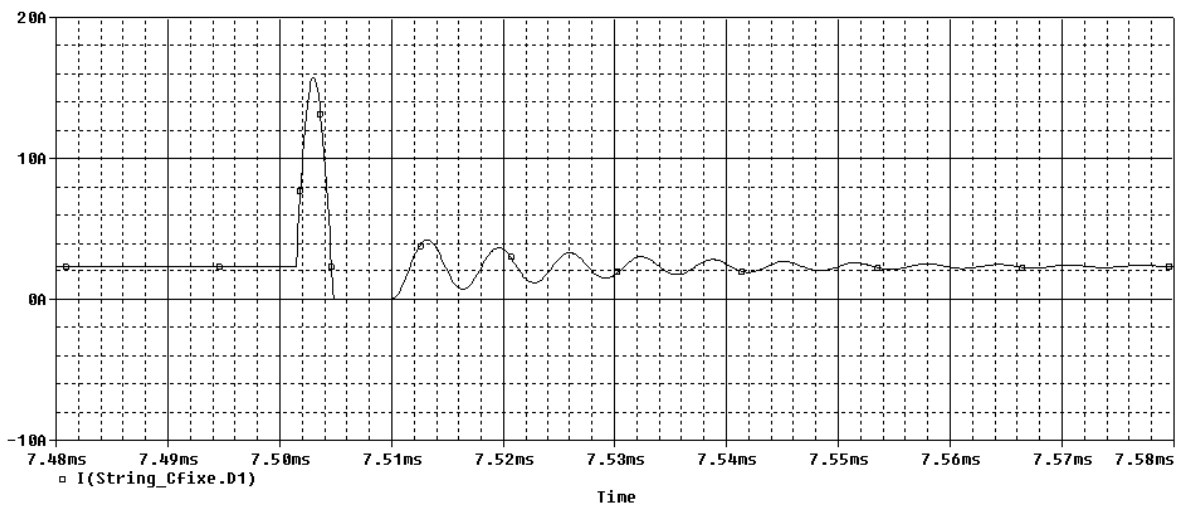


Figure 3.4-1 : Current at shunt closure at section output

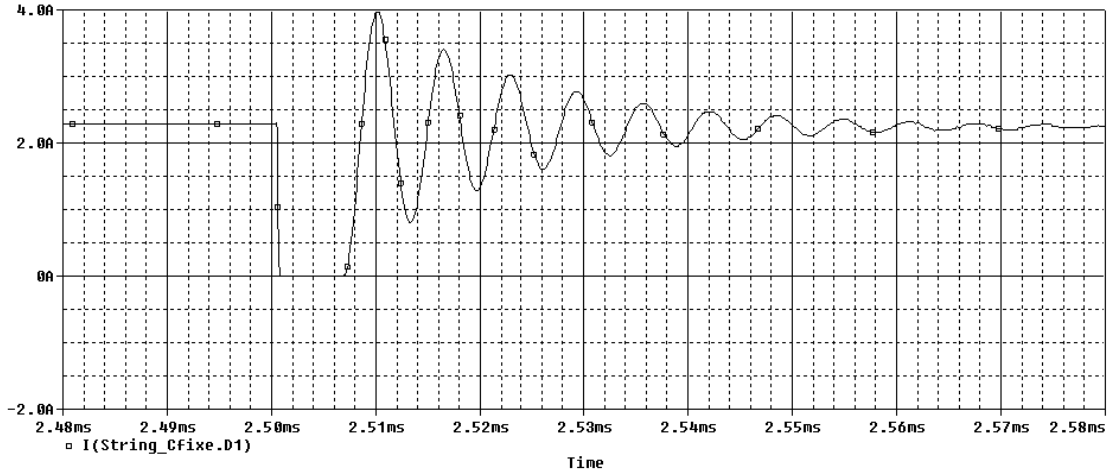


Figure 3.4-2 : Current at shunt opening at section output

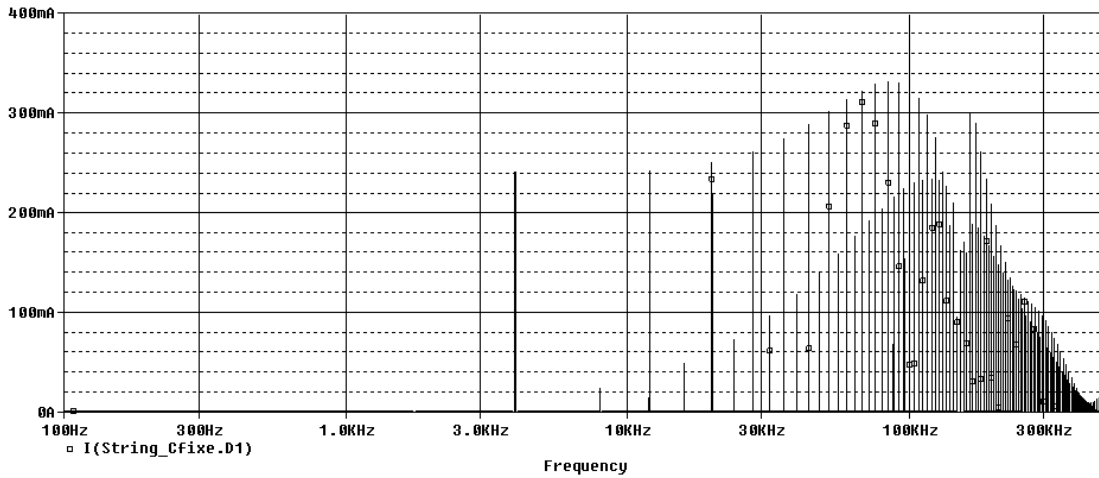


Figure 3.4-3 : Fourier transform of current at shunt opening and closure



The analysis of the results obtained at shunt closure (figure 3.4-1) shows that the values are similar to the measurements performed for the solar array section capacitance (see annex 4).

As the section contains 5 identical strings, we can consider that the transient amplitude at string level is the transient amplitude at section level divided by 5.

In fact as the solar array capacitance is distributed along the strings, the transient at string level output is the maximum value. However as the loops formed by the two current paths (main and redundant) a large part of the loop being constituted of wires, we can consider that the error will be lower than 25 % if the maximum value is taken into account.

In time domain the transient value reaches 15 A at section level, it conducts to a value of 3 A at string level, and 1.5 A at half string level.

In frequency domain the same approach can be considered, it conducts to have a maximum value of $330 \text{ mA}/(2 \cdot 5) = 33 \text{ mA}$ at 90 kHz.

3.4.2.1 Magnetic field of Section 30 at point E

The evaluation of the field generated by section 30 at point E level is performed taking into account the following values :

$$I = 0.033 \text{ A at } 90 \text{ kHz}$$

$$R = 0.44 \text{ m}$$

$$D1 = 0.294 \text{ m}$$

$$D2 = 0.512 \text{ m}$$

$$\text{The result is } B_x = 5.02 \text{ nT and } B_r = 14.77 \text{ nT}$$

$$\text{Field amplitude is } B = 15.6 \text{ nT i.e. } 84 \text{ dBpT}$$

3.4.2.2 Magnetic field of section "X" at point "Y"

All fields shall be evaluated following the same approach as in § 3.4.2.1. This conducts to increase by 3.3 dB (corresponding to the ratio of the currents) the results in dBpT of the last column of the table in § 3.4.1.2.



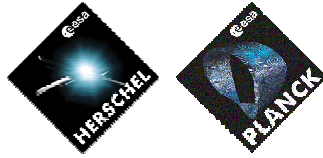
4. ANALYSIS

The magnetic fields generated by the Herschel solar array sections on PACS cryo-harness have been evaluated, results are summarised in the following table :

Solar array section N°	Field at S3R switching frequency (dBpT)	Field at 90 kHz (dBpT)
29	35	38.3
17	44	47.3
28	45	48.3
11	47	50.3
9	47	50.3
20	48	51.3
18	51	54.3
16	52	55.3
1	52	55.3
14	54	57.3
23	54	57.3
3	55	58.3
24	58	61.3
6	58	61.3
21	58	61.3
7	58	61.3
8	58	61.3
4	58	61.3
22	58	61.3
12	59	62.3
15	59	62.3
19	60	63.3
26	66	69.3
25	67	70.3
27	68	71.3
10	68	71.3
13	74	77.3
30	81	84.3

By doing a cross check with the values evaluated in the frame of other programs (see annex 3 and 5), the order of the values obtained is correct. An error lower than 10 dB can be considered.

Considering section 30 and point E, the distance between them is low and explains the high value of the magnetic field obtained.



An other aspect which have to be considered is that PACS sensors can be sensitive in a large frequency band (e.g. some hundreds kHz). It can be of interest to perform a test with a time domain transients at the S3R switching rate .

5. CONCLUSION

The solar array is compliant with its magnetic moment requirement of 1 Am². However, magnetic field values of 84 dBpT can be generated by the Herschel solar array on the PACS cryo-harness.

The radiated susceptibility tests performed on Herschel EQM have shown the following susceptibility levels for PACS photometer :

90 dBpT from 30 Hz up to 20 kHz

80 dBpT from 20 kHz up to 50 kHz

This is in deviation w.r.t. the radiated susceptibility H-field requirement (EMCEQ-250 of [RD03]) which asks for 140 dBpT susceptibility level between 30 Hz and 50 kHz (see H-P-PACS-RFW-004).

Considering the worst case, we have no margin between the susceptibility level and the field generated by the solar array at point E level. Taking into account a value of 70 dBpT, at least 6 sections can be considered as critical.

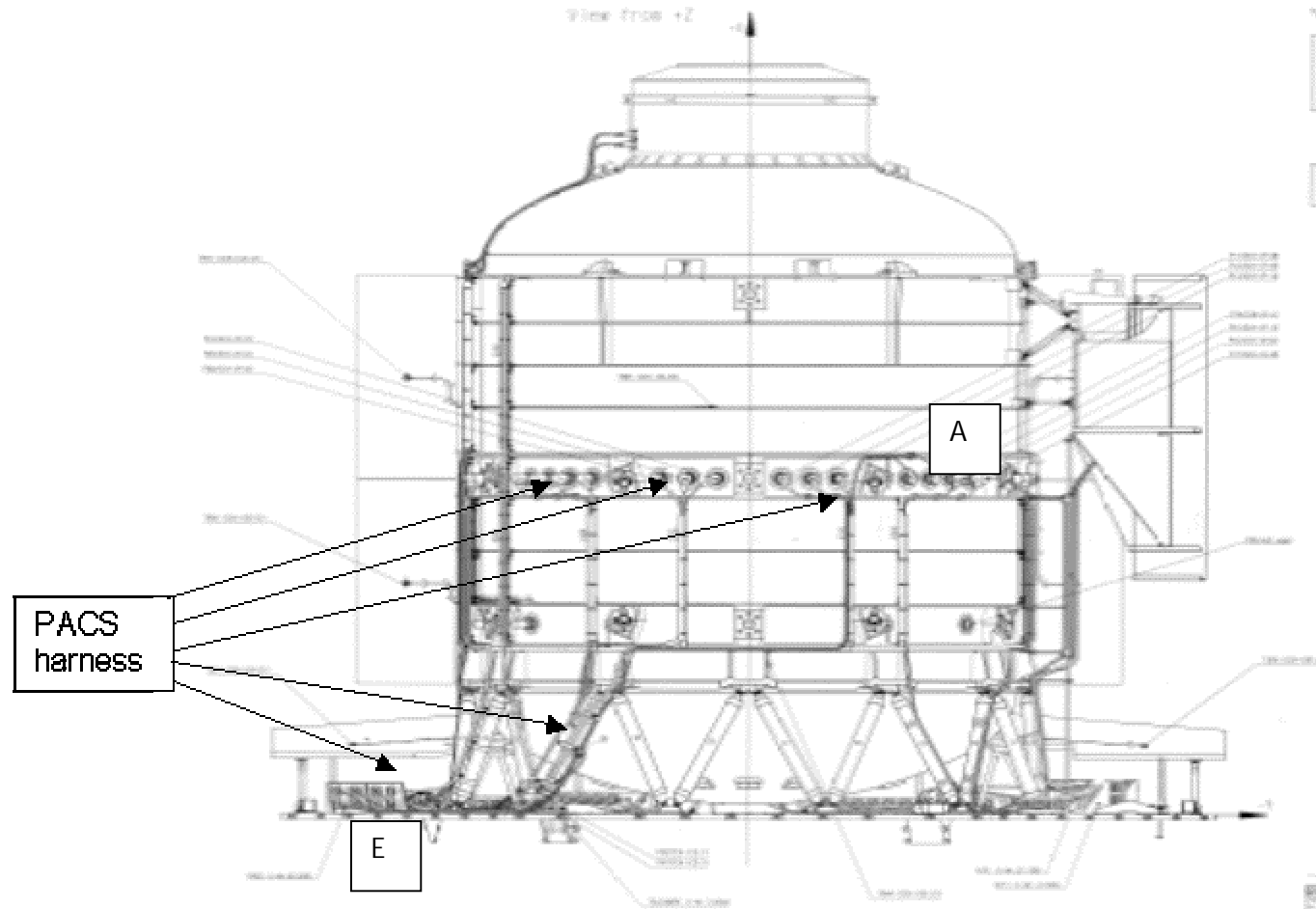
Some modifications are proposed in [RD 07] technical note.

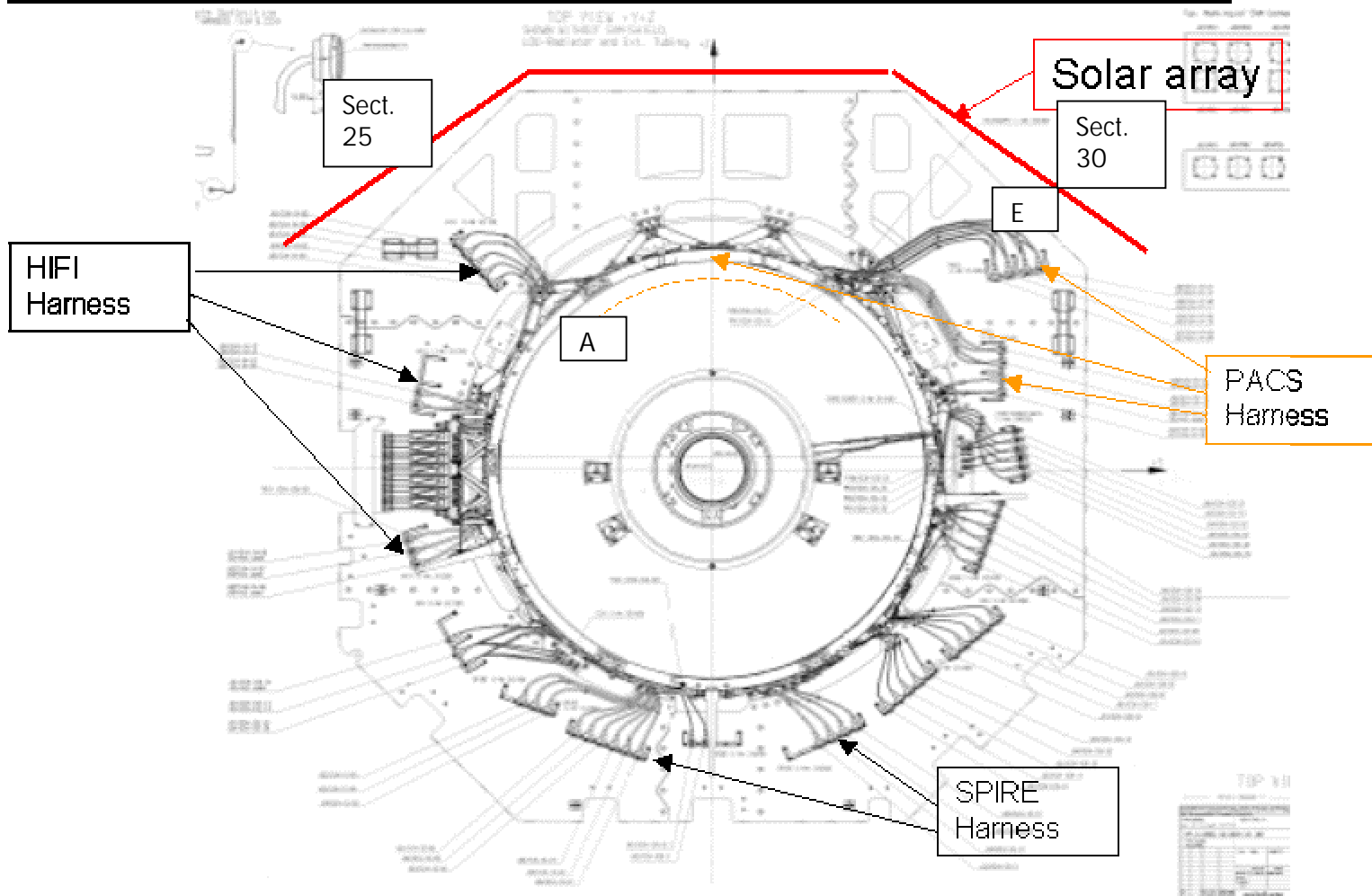
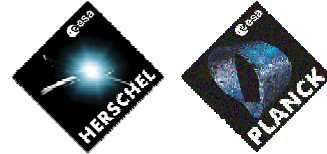
In order to check at FM satellite level the compatibility between Solar Array and PACS, it is proposed to add to the radiated susceptibility test a time domain injection of the magnetic field at most critical points close to the cryo-harness.

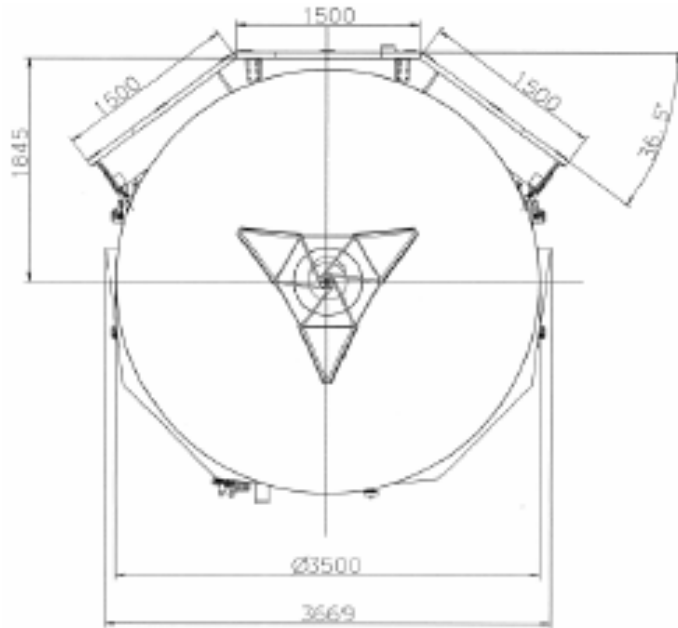
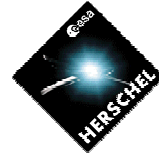
Note : The magnetic field generated by the Herschel solar array on the SPIRE cryo-harness is very low due to the fact that the cryo-harness is located on the opposite side with regard to the solar array (taking the section 30 with a distance of 2 m, the magnetic field at cryo-harness level is lower than 0.3 nT, i.e. 50 dBpT).

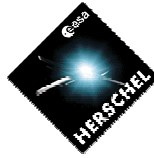


APPENDICES : 1
HERSCHEL Mechanical layout









APPENDICES : 2

Measurement and simulation of the current variation in the solar array during shunt switching



Coupled tests between solar strings and a Sequential Switching Shunt Regulator

To analyse the influence of the solar array capacitance on the behaviour of the power conditioned electronics, coupled test between one string and a S3R has been realized. The electrical scheme with a string composed of 273 non-IBF silicon Sharp 100 μ m/2ohm cells is displayed Figure 2.

This string under test is composed of 7 small strings ; for each string, cells are matched at 1% but the different strings are not matched; they have different grades. The panels are connected to ground via a 20k Ω resistance. A free wheel diode may be also connected in parallel with the string. A flasher illuminates the cells during several milliseconds. Several measurements are recorded on an oscilloscope (SA current, SA voltage, S3R voltage, differential voltage of each section). Different parameters (length of the harness, number of cells, lighting incidence, commutation frequency) were modified in order to analyse their influence on the transients.

A detailed PSpice model of the coupling of the solar array and the S3R has been elaborated and correlated with these tests.

One solar cell is modelled as shown on Figure 1, this model taking into account the variation of the silicon solar cells parasitic capacitance C_p with the voltage cell.

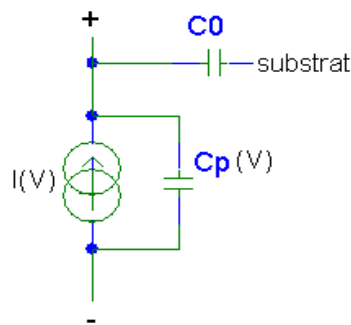


Figure 1 : Solar cell modelisation

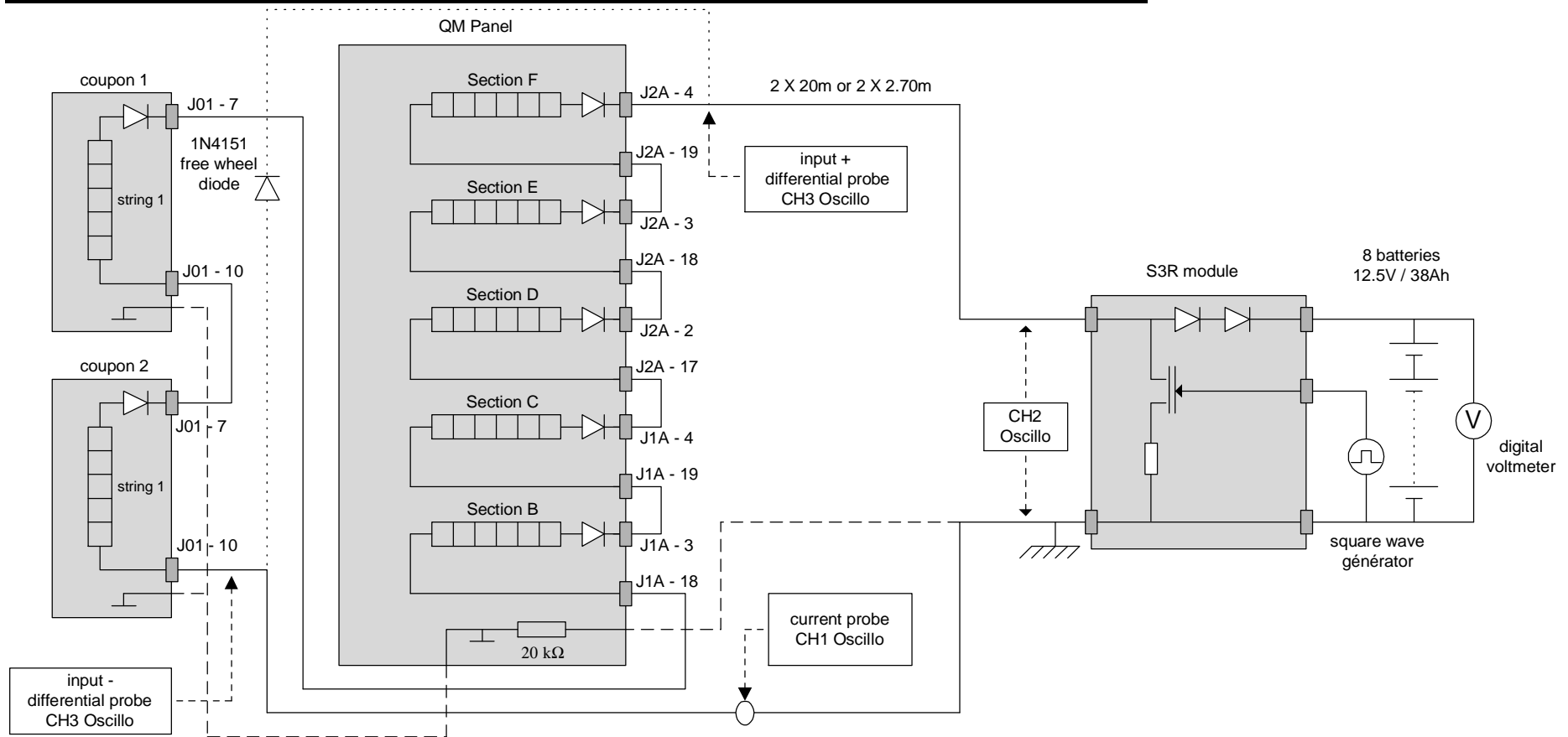
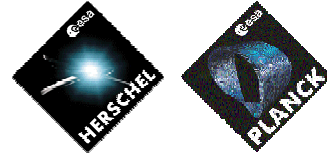
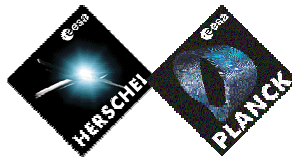


Figure 2 : Test electrical scheme



The dynamic behaviour of one string is determined by analysing the parasitic capacitance network of n solar cells in series.

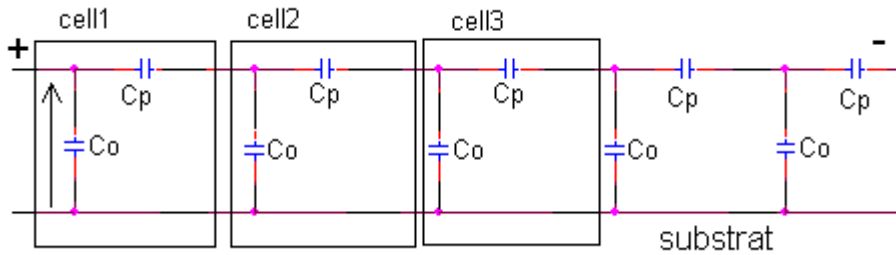


Figure 3 : String capacitive network

If all the parasitic capacitances C_p are equal, the string can be considered as a chain of n identical quadripoles.

The model of one string is thus presented Figure 4, R_{cell} being the cell inter-connexion resistance, the capacitances $C_{+/-}$, C_{sub+} and C_{sub-} of the string being a function of the capacitances values C_p and C_0 and of the number of solar cells.

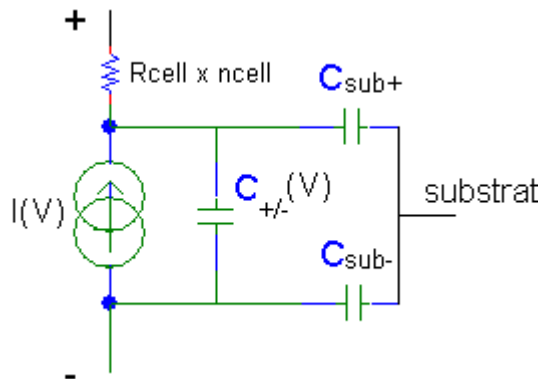


Figure 4 : Solar string modelisation

In the test Pspice model, the parameters of each small string have been adjusted in order to take into account the dis-matching between the strings. Indeed, as the strings were not perfectly matched, the voltage sharing was not uniform. Some cells were reversed polarised during shunt closure as shown on Figure 5.

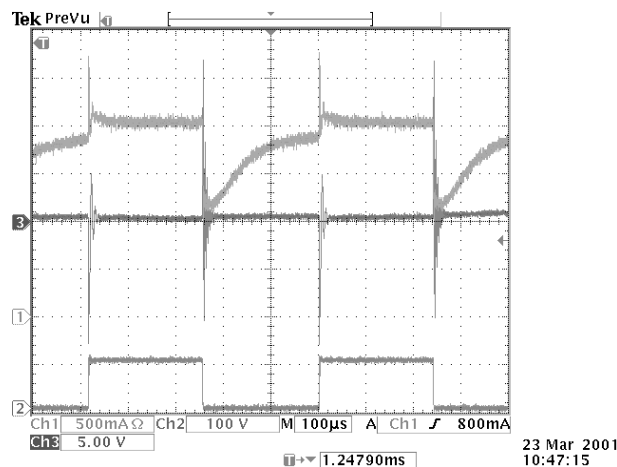
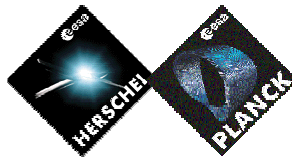
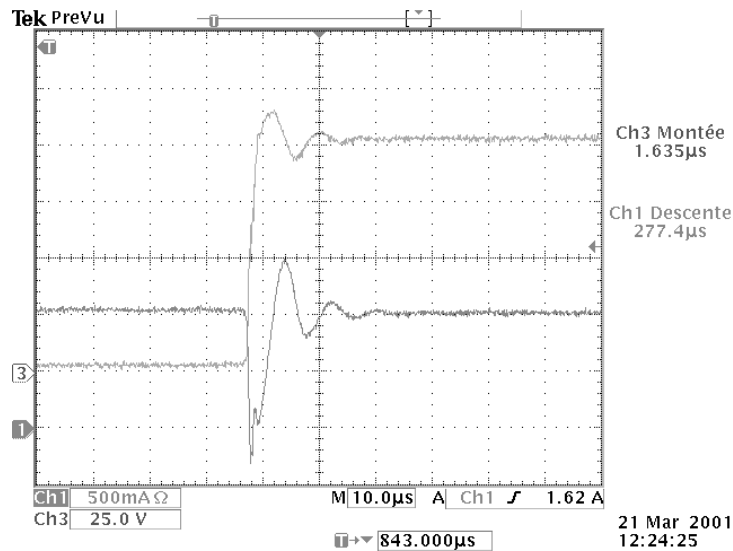


Figure 5 : Differential voltage string E



These Pspice simulations have been correlated with the experimental results as shown Figure 6 and Figure 7. This model has then been used to predict current and voltage transients due to shunt regulation for in flight configurations.



Ch1 : string current (500mA/div)
Ch3 : string voltage (25V/div)

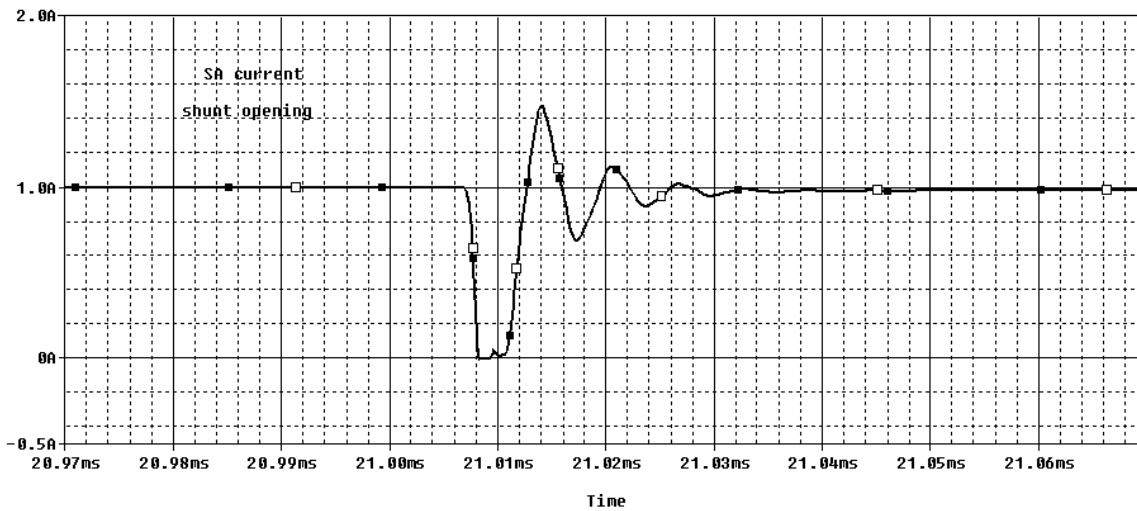
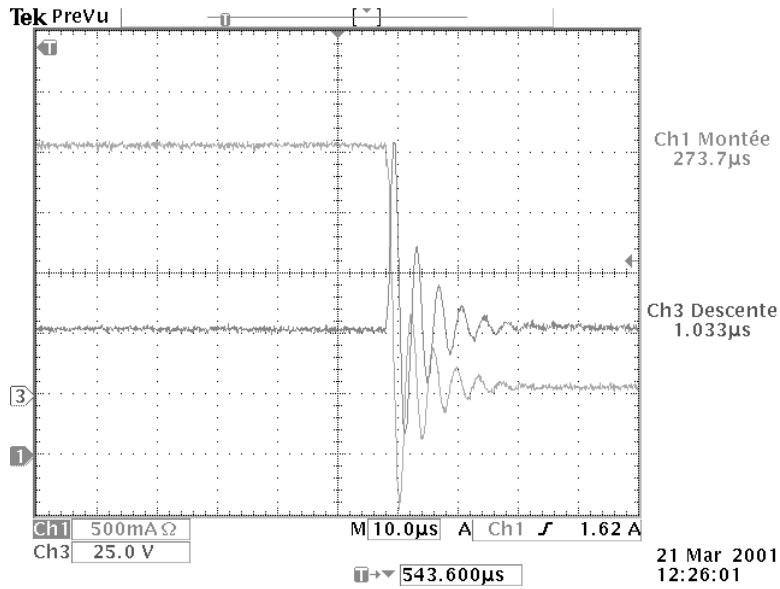
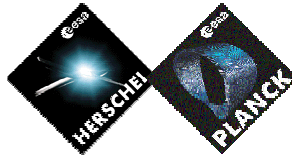


Figure 6 : Current transient at shunt opening (test and simulation)



Ch1 : string current (500mA/div)
Ch3 : string voltage (25V/div)

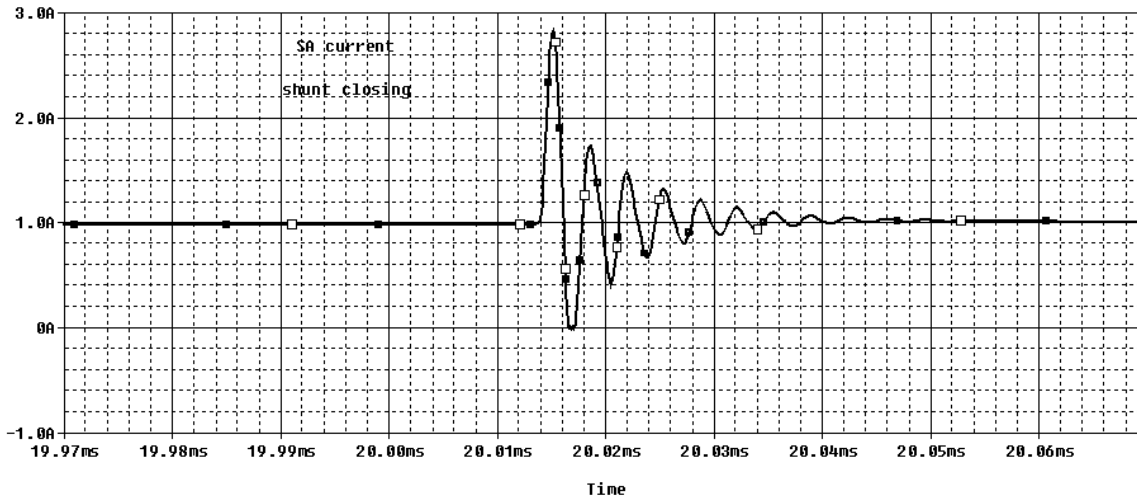
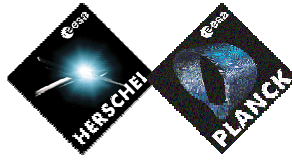


Figure 7 : Current transients at shunt closing (test and simulation)



APPENDICES : 3

Magnetic field evaluation on MSG

Main results of the evaluation of the magnetic field generated by the solar array of MSG are presented in this annex.

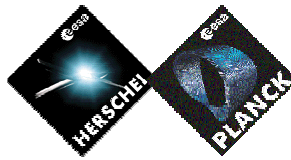
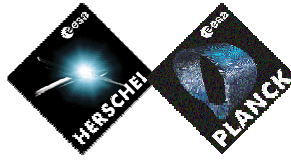


Table 7.2-6: Summary of Simulation Results

UNIT	FIELD STRENGTH			
	Distance from S/A	H [dB μ V/m] at 14 kHz	E [dB μ V/m/MHz] at 14 kHz	D [dBpT] at 4 kHz
PRU	0.49 m	63.9	111.9	39.7
PCU	0.21 m	77.8	125.8	61.0
AOCE	0.31	48.4	96.3	66.9
ACU	0.07	118.5	166.5	98.1
GERB (OU)	0.13	83.3	131.3	71.6
GERB MEC	0.29	57.0	105.0	42.5
CDMU	0.53	48.8	96.8	47.2
FPCA	1.6	-58.5	-18.7	50.2
1m from S/A, 45°	1	26.0	73.9	25.2
1m from S/A, 60°	1	12.7	60.7	9.1
1m from S/A, 112.5°	1	24.8	72.8	28.9
1 m from S/A, 135°	1	32.7	80.7	34.5
1m from S/A, 157.5°	1	38.9	84.8	35.0
1 m from S/A, 180°	1	38.2	86.2	37.0



Radiated Emissions, B-Field NB

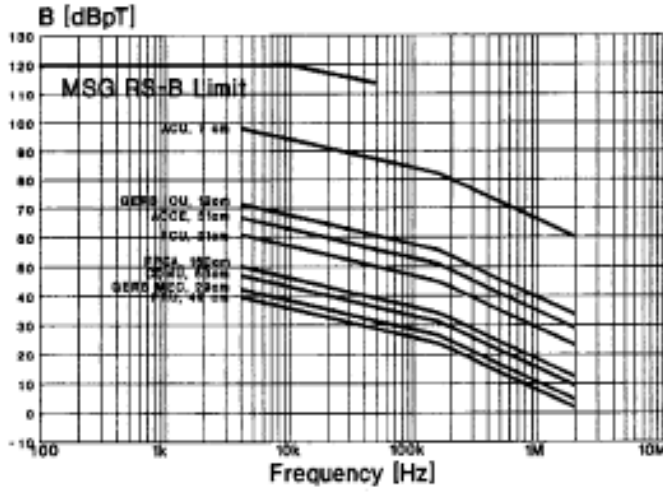


Fig. 7.2-14: Magnetic Fields at the respective Units

Radiated Emissions, B-Field NB

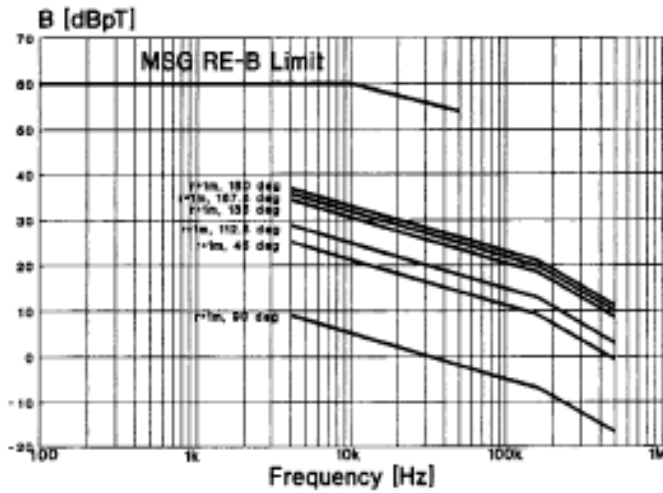
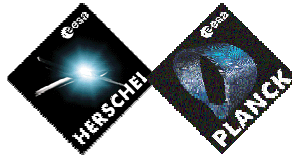


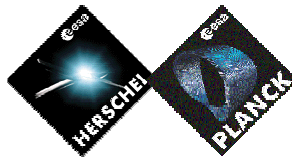
Fig. 7.2-15: Magnetic Fields at 1 m Distances



Appendices : 4

Solar Array Section Capacitance measurement on Planck

Results of the solar array section capacitance measurement performed on Planck are presented hereafter. They are extracted from [RD 02].



Capacitance / Inductance TEST

General Note :

The voltage profile cannot be represented as a simple charging of a capacitor by a constant current.

The presence of the blocking diodes (in series with the strings) cause an initial oscillation (due to the small capacitance of the diodes), being the time constant of this transient lower than the one dominated by the capacitance of the solar cell.

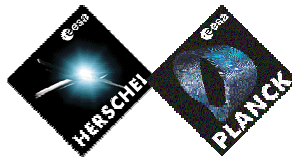
The results are confirmed also by the opposite transition, in which we can derive the same values of the dynamic parameters.

Item	Irradiance	String Current (Isc)	String Voltage (Voc)	rise time 20-80%	ΔV (20-80%)	Ccells
Section 10 (4 strings)	100 SC	2 A	57 V	7 μ s	34 V	410 nF

Item	Series resistance (Rs)	Period of oscillation (Trep)	Decay constant (τ)	Inductance (L)	Cblocking
Section 10 (4 strings)	$\cong 1 \Omega$	160 ns	$\cong 05 \mu$ s	250 nH	2.6 nF

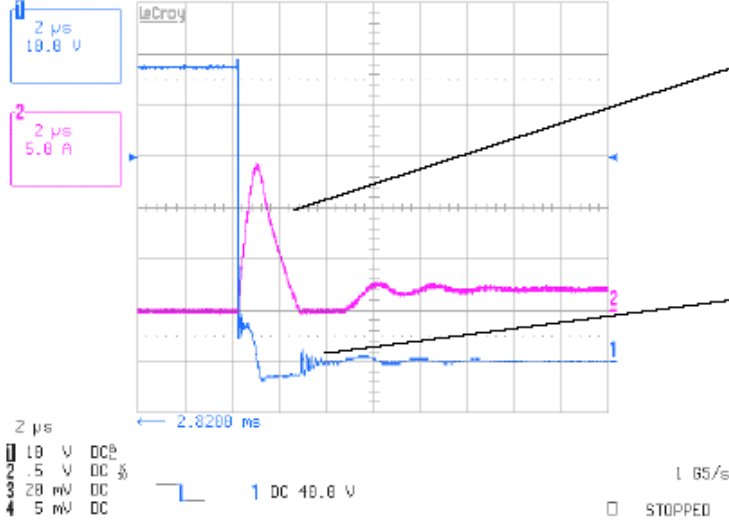
Item	Irradiance	String Current (Isc)	String Voltage (Voc)	rise time 20-80%	ΔV (20-80%)	Ccells
Section 11 (5 strings)	100 SC	25 A	57 V	7 μ s	34 V	410 nF

Item	Series resistance (Rs)	Period of oscillation (Trep)	Decay constant (τ)	Inductance (L)	Cblocking
Section 11 (5 strings)	$\cong 1 \Omega$	160 ns	$\cong 05 \mu$ s	250 nH	2.6 nF



Section 10 test results :

3-Feb-06
13:47:45

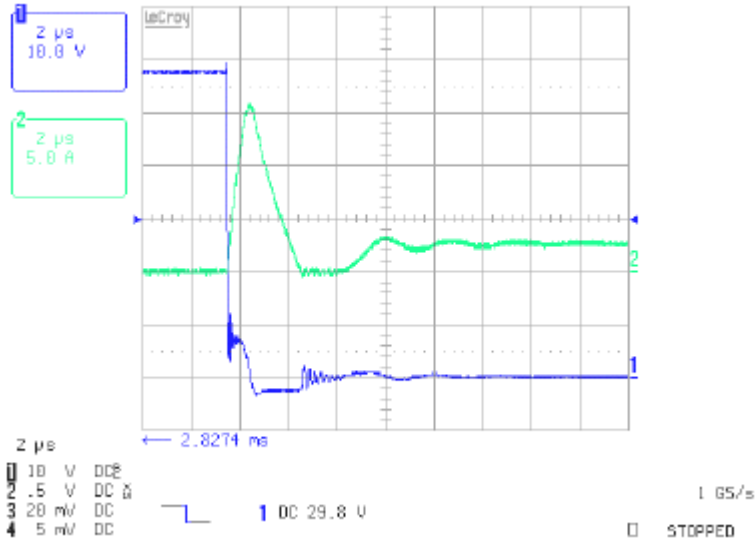


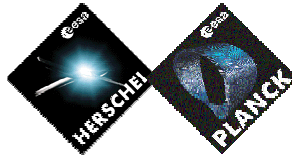
*Ccell is prevalent
The valid relation is:
 $T_{REP} = 2\pi\sqrt{LC_{cell}}$ (1)*

*Diode is blocking the negative wave
Cdiode is prevalent.
The valid relation is:
 $T_{REP} = 2\pi\sqrt{LC_{blocking}}$ (1)*

Section 11 test results :

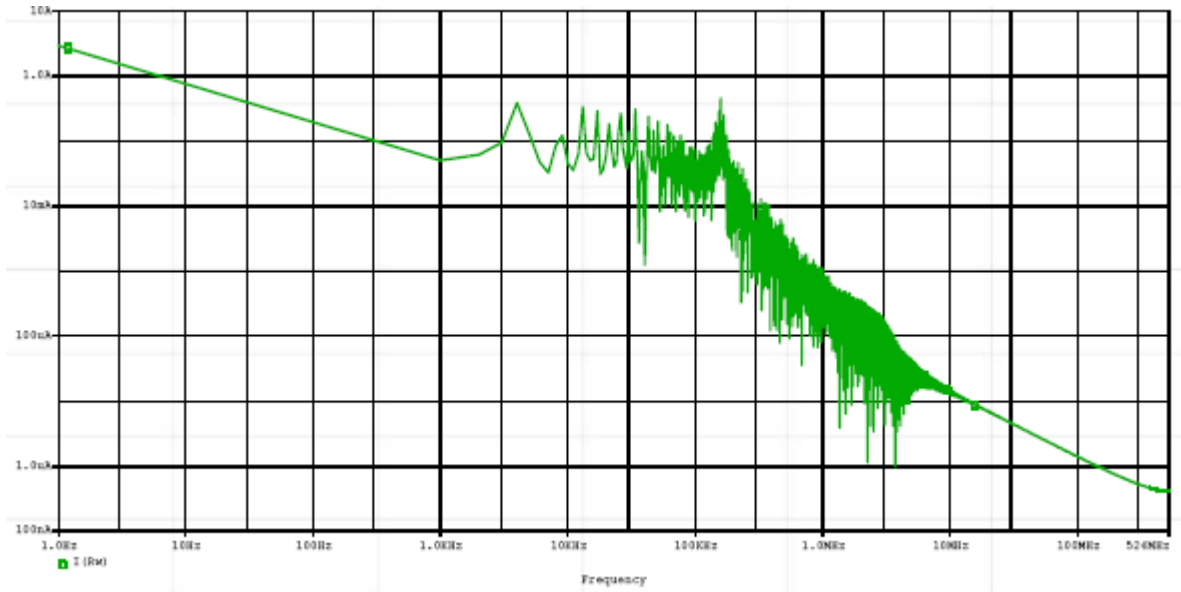
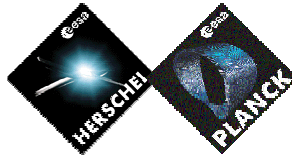
3-Feb-06
11:41:11





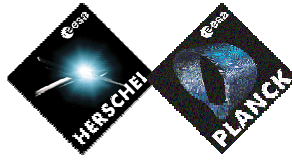
APPENDICES : 5

Results of simulations performed by a supplier in the frame of an other program



Results of an analysis performed with the following parameters :

- Section current : 3 A
- Harness inductance : 2 μ H
- Section capacitance : 500 nF



END OF DOCUMENT